Journal of The
Electrochemical Society

Gas Crossover in Membrane Electrolyzers—The Impact of MEA Conditioning on Gas Permeability

To cite this article: Leander Treutlein *et al* 2025 *J. Electrochem. Soc.* **172** 064507

Journal of The Electrochemical Society, 2025 **172** 064507

Gas Crossover in Membrane Electrolyzers—The Impact of MEA Conditioning on Gas Permeability

Leander Treutlein,[1,2,z] Ali Javed,[1] Niklas L. Wolf,[1,2] Hans Kungl,[1] André Karl,[1] Eva Jodat,[1] and Rüdiger-A Eichel[1,2,3]

[1]*Institute of Energy Technologies, Fundamental Electrochemistry (IET-1), Forschungszentrum Jülich, 52425, Germany*
[2]*Institute of Physical Chemistry, RWTH Aachen University, D-52062 Aachen, Germany*
[3]*Faculty of Mechanical Engineering, RWTH Aachen University, D-52062 Aachen, Germany*

Hydrogen crossover in proton exchange membrane electrolytic cells (PEMEC) can lead to reduced usable hydrogen output, shortened lifespan, and interruptions in operation due to safety concerns. Extensive studies have explored the crossover mechanism under various operating conditions using different setups. In this study, we demonstrate a setup that is capable of quantifying hydrogen and oxygen permeability of dry and wet membranes, as well as catalyst coated membranes; i.e. membrane electrode assemblies (MEAs). We monitored the hydrogen and oxygen permeabilities of Nafion™ N115, N117 and NR212 membranes, respectively, and studied the effect of catalyst coating on hydrogen permeability of the membrane. The impact of conditioning on N115-based MEAs in a fully hydrated state was investigated. To realize this, MEAs were subjected to various conditioning protocols; break-in (applied current), in situ vs ex situ pre-treatment (water exposure), and elevated vs lowered temperature pre-treatment, which revealed a significant influence on hydrogen permeability.
 [DOI: 10.1149/1945-7111/ade00f]

Manuscript submitted December 31, 2024; revised manuscript received May 12, 2025. Published June 11, 2025. *This paper is part of the JES Focus Issue on Proton Exchange Membrane Fuel Cell and Proton Exchange Membrane Water Electrolyzer Durability III.*

To combat the rising levels of CO_2 in the world's atmosphere, the European Union has set a target: to be the first carbon neutral continent by the year 2050. Decarbonizing all energy sources is key for reaching this goal, and a prospective approach might be harnessing pure hydrogen as an energy source.[1] Water electrolyzers offer a way to transform green energy sources to green hydrogen. Of the available technologies, proton exchange membrane electrolytic cells (PEMECs) offer high current densities and transient system operation, making it an ideal match for intermittently available renewable energy sources.[2–4] However, the technology of PEMECs is still ramping up.[5] To mitigate the potential challenges associated with the widespread implementation at industrial scale, aging and degradation mechanisms of PEMEC components have to be investigated.[6,7] Most recently, various observations at the catalyst layer,[8–12] porous transport layers (PTLs)[13–16] and at the membrane level have been reported.[17–21]

The membrane is considered one of the most critical components of a PEMEC, as it significantly affects the efficiency and lifespan of the system.[17,19,22,23] During the operation, the membrane is subjected to chemical, thermal, and mechanical stresses, which can lead to membrane thinning.[24–28] This process involves a reduction in the total thickness of the membrane and the loss of ionomer material. Consequently, the ohmic resistance across the membranes is decreased, while the rate of gas crossover increases. Gas crossover is typically defined as the process of oxygen passing from the anode to the cathode, or hydrogen passing from the cathode to the anode, thereby decreasing the purity of the generated gases. This process reduces the total efficiency of the electrolytic system, not only due to gas loss but also via the recombination of hydrogen and oxygen to water when they mix. Another result of gas crossover is the chemical degradation of the membrane. The most widely accepted pathway for this degradation is the formation of hydrogen peroxide, which can further produce radicals in the presence of metal cations. These radicals, subsequently, attack the polymer of the membrane, leading to an autocatalytic effect wherein the membrane becomes thinner, with the crossover rate increasing in return.[6,25,26]

Detailed investigations have been done to understand the mechanism of gas crossover, with an emphasis on Nafion™, as it is the most frequently used ionomer in PEM fuel cells and PEM electrolyzers.[20,21,29–31] Comparing this literature data shows a significant variation in the permeability of both oxygen and hydrogen, up to tenfold, even using the same membrane. The differences arise from varying operating temperature, measurement technique or hydration status of the membrane. The water content of Nafion™ is strongly influenced by its pre-treatment,[32,33] which in response affects the gas permeability, since it depends on the hydration state of the membrane.[34] Even, during the operation of PEMECs and fuel cells, an increase in the hydration level and changes in the morphology of Nafion™ can occur.[35,36] Consequently, an investigation is needed to show the origin of the disparity in literature data. A specialized experimental setup is required that allows to measure permeability of membranes and membrane electrode assemblies under varying temperature and humidity, as well as in situ measurement after pre-treatment and electrolysis, to not alter the sample.

The available literature shows a variety of measuring approaches to investigate hydrogen and oxygen crossover in PEMECs. One approach makes use of crossover sensing by electrochemical detection, requiring a special cell design[34,37,38] and specific operating conditions, making a comparison to real operating electrolytic cells difficult. Another experimental approach entails the monitoring of hydrogen in oxygen in the exhaust stream during electrolysis operation.[39,40] With this technique, the impact of different operating conditions on hydrogen permeation, crossover mechanisms, and also possible mitigation strategies can be investigated. While the operating conditions are comparable to a real-world scenario using this technique, it is not optimal for examining catalyst-free membranes, primarily because electrolysis operation must have catalysts on both sides of the membrane. The time lag method,[36,41] which requisites for a sophisticated apparatus with vacuum, and the volumetric method,[35] which may be affected by water vapors when measuring wet samples, have also been employed for evaluating gas crossover. Other studies have shown the potential use of gas analyzers, gas chromatographs or other detectors at the exit stream of the measuring cells.[42–45]

This study quantifies hydrogen and oxygen permeability of dry and wet Nafion™ membranes, as well as membranes with catalyst coating known as membrane electrode assemblies (MEAs), employing a setup reported recently.[46] The specialty of this setup is that

[z]E-mail: l.treutlein@fz-juelich.de

it allows in situ measurement of gas permeability pre- and post-operation of PEMEC without first disassembling the cell to get to the MEA. Thereby, this allows to study the effects of pre-treatment (treating membrane or MEA before cell assembly; ex situ pre-treatment, or after cell assembly; in situ pre-treatment) or break-in (activating MEA; the membrane and catalyst by electrolysis) on gas permeability. The overarching term for both (break-in and pre-treatment) is defined as conditioning.[47] By applying different in situ and ex situ pre-treatment, and breaking-in procedures on Nafion™ based membranes and MEAs, this study finds a non-negligible effect on hydrogen permeability. This can partially explain the disparity found in literature, as pre-treatment and break-in procedures are inconsistent, unstated, neglected or excluded. The conditioning procedures explored in this work highlight the impact on hydrogen permeability of PEMECs.

Experimental

Membrane pre-treatment and MEA conditioning.—Commercially available Nafion™ membranes in activated H^+-form with different thicknesses N115 (wet: 170 μm, dry: 127 μm), N117 (wet: 210 μm, dry: 182 μm) and NR212 (wet: 90 μm, dry: 50 μm), and HYDRion™ membrane electrode assemblies (MEAs), all from Ion Power, with an active area of 25 cm^2 were used in this experimental study. The H^+-form was chosen, as it is suitable for water electrolysis and only little difference in comparison to the K^+-form is to be expected.[35] The MEA consists of Nafion™ N115 as the membrane, platinum with a loading of 0.3 mg cm^{-2} as the cathode catalyst, and iridium oxide with a loading of 1 mg cm^{-2} as the anode catalyst. The membranes were conditioned via a pre-treatment procedure at 80 °C for 24 h in a beaker containing deionized water (DI-water) before assembling into the PEMEC (ex situ pre-treatment). N115-based MEAs were subjected to conditioning by pre-treatment or break-in protocols, as listed in Table I. The MEAs were pre-treated either before cell assembly (ex situ pre-treatment) or after cell assembly (in situ pre-treatment). MEA 1 and MEA 4 were conditioned via in situ pre-treatment and break-in procedures, respectively. Moreover, respective cells were not disassembled throughout the conditioning process to avoid any potential damage to membrane or alterations in applied compression. The ex situ pre-treatment was applied to MEA 2 and MEA 3. The thickness of the membranes and the MEAs (including both electrodes) was measured using a foil thickness gauge (Käfer FD 1000/30−3) after all tests were conducted. This thickness is considered to represent the thickness of the membrane or MEA inside the cell assembly during measurement and was used to calculate permeability.

Cell preparation.—An in-house built single PEM electrolytic cell with 4.4 cm × 4.4 cm active area was used for this experimental study. The endplates were composed of stainless steel, while flow field plates were fabricated from grade 2 titanium. Anode and cathode flow field plates were coated with platinum and gold, respectively. On the cathode side, titanium gauze (Fisher Scientific Mesh 40) porous transport layer (PTL) with one carbon sheet (Toray TGP-H-60) was used. On the anode side, one layer of expanded metal titanium with platinum coating (MeliCon MELIDFF) was utilized as the PTL. Gaskets were made from PTFE, using a thickness chosen to be 100 μm thinner than the cathode PTL to reach ∼50% compression of the carbon paper. The cell was clamped by 8 M5 bolts, each of which was tightened with a torque of 5 Nm.

Setup.—To quantify hydrogen and oxygen crossover, a setup was employed[46] with the intent of measuring dry or wet membranes, as well as MEAs, without disassembling the PEMEC after conditioning. This approach prevents the membrane or MEA from getting damaged during disassembly of the cell and avoids any possible changes in the applied compression force. Moreover, gas crossover in PEMECs can be directly quantified pre- and post-operation. Therefore, this setup can be used along with an electrolysis test station to measure the permeability of MEA without disassembling the measurement cell. These characteristics enable a realistic comparison of different conditioning procedures, applied in this work on different membranes and MEAs. Figure 1 demonstrates the measurement principle of the setup employed in this study. On side of the electrolysis cell is flushed with either hydrogen or oxygen (testing gas) and the other is flushed with argon (carrier gas) with a known flow rate. During measurement the testing gas is pressurized, and the test cell is heated to a set temperature. The gas passes through the membrane via diffusion into the carrier gas stream; carrying it further into the gas analyzer. After detecting the permeated gas through the membrane or MEA via thermal conductivity detector, permeability was calculated using the Eq. 1, where L is the thickness of the sample, e_{H2} is the molar flow rate of hydrogen or oxygen from one side of the cell to the other, and p_{H2} is the hydrogen partial pressure:

$$\varepsilon_{H2} = \frac{L \cdot e_{H2}}{p_{H2}} \quad [1]$$

Figure 2 illustrates P&ID diagram of the presented setup, highlighting all of its components required for a gas crossover experiment. The gases flowing into the system were regulated by mass flow controllers (Argon: Bronkhorst F-201CV, Oxygen and Hydrogen: Sensirion SFC5500). The cathode side of the cell can

Table I. Conditioning protocols applied on N115-based MEA samples. For MEA 1 and MEA 4, the cell was not disassembled between the steps. MEA 2 and 3 were pre-treated before assembling into the test cells.

Conditioning			
Pre-treatment		Break-in	
	Ex-situ		
In-situ MEA 1	MEA 2	MEA 3	In-situ MEA 4
• 24 h at 30 °C	10 min at 80 °C	24 h at80 °C	• 24 h at 1 A cm^{-2} at 60 °C
• 10 min at 80 °C			• 24 h at 2 A cm^{-2} at 60 °C
• 24 h at 80 °C			• 24 h at 3 A cm^{-2} at 60 °C
Permeability measured after each treatment			

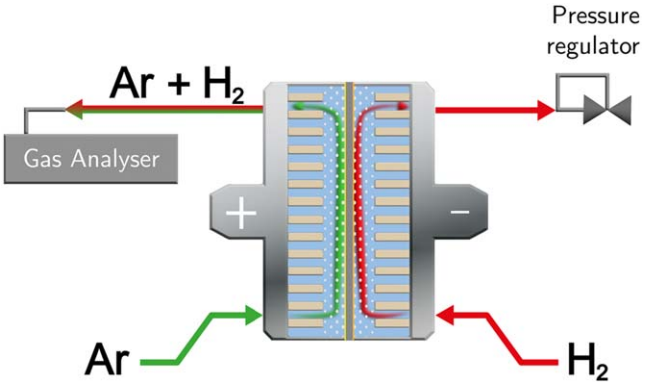

Figure 1. Schematic diagram of the gas crossover through the membrane or MEA in an in-house built proton exchange membrane electrolytic cell, depicting only the hydrogen crossover test. Hydrogen is pressurized by the pressure regulator. Hydrogen then permeates to the other side of the cell, where it is caried by the argon gas stream to the gas analyzer, allowing for the detection of the amount of hydrogen.

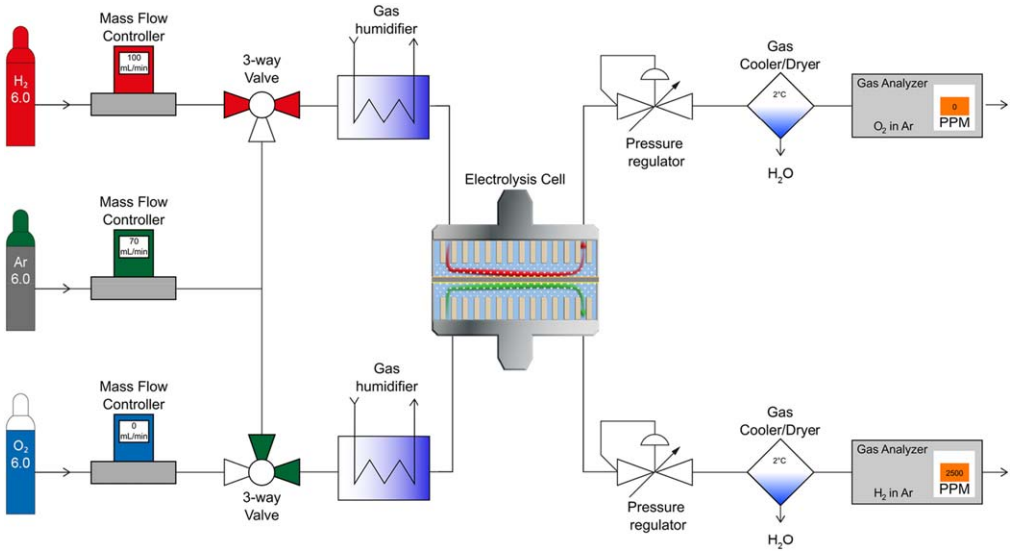

Figure 2. Layout of the gas crossover setup, the gas flow is from left to right. The scheme displays the gas supply with mass flow controllers (MFC), gas humidifiers, measurement cell, pressure control, dehumidifiers, and gas analyzers from left to right.

be flushed by argon or hydrogen, and the anode side by argon or oxygen. The gas supplied to the cell was humidified by membrane humidifiers (Permapure MH-110-42), and the dew point of the gases was regulated by the water temperature flowing through the humidifier. A dew point above the cell temperature not only stops the membrane from drying out but also leads to water condensation. This is because the gas is already fully saturated, ensuring proper hydration during all measurement steps. To limit the amount of liquid water inside the cell, the humidifiers were always kept at 5 K over the temperature of the measurement cell. Back pressure regulators (Equilibar ZF-Series) were used to set the pressure of the permeate inside the cell. Before measuring the concentration of permeate (in this work hydrogen or oxygen) in the carrier gas, gases were dried by a gas cooler (M&C Techgroup ECP2000) to 2 °C. This ensures that the gas has always the same humidity when it enters the gas analyzer. The detection of hydrogen in argon or oxygen in argon was achieved with thermal conductivity detectors (Messkonzept FTC320) employed for each side of the PEMEC. Before each measurement, the whole setup was flushed with argon at a flow rate of 200 mL min^{-1}. For gas crossover experiments, the flow rate of argon was set to 70 mL min^{-1} and hydrogen or oxygen 200 mL min^{-1}, respectively.

Results

The permeabilities of Nafion™-based membranes and MEAs were investigated by measuring the gas permeation using argon as a carrier gas. Figure 3 shows the quantity of hydrogen permeating through a N115 membrane at different temperatures under fully humidified conditions. The permeation measurements were initiated after the flushing cycle, which required 125 minutes. Since temperature and hydrogen passing through the membrane required some time to stabilize, each data point was acquired after an equilibration time of 20 minutes. Black arrows in Fig. 3 denote the data points used to calculate the permeation and subsequently permeability. As gas diffusion is a thermally activated process, the membrane shows an increase in permeation with increasing temperatures ranging from 40 °C to 80 °C (1607 ppm to 3056 ppm).

Hydrogen and oxygen permeability measurements were performed on N115, N117 and NR212 Nafion™ in both wet and dry conditions. Pristine membranes were submerged in 80 °C water for 24 h before cell assembly (ex situ pre-treatment). Similarly, for the dry measurements, pristine membranes were dried at 80 °C with a continuous flow of argon. For all the membranes both in wet and dry state, Fig. 4a shows the hydrogen permeabilities, whereas Fig. 4b

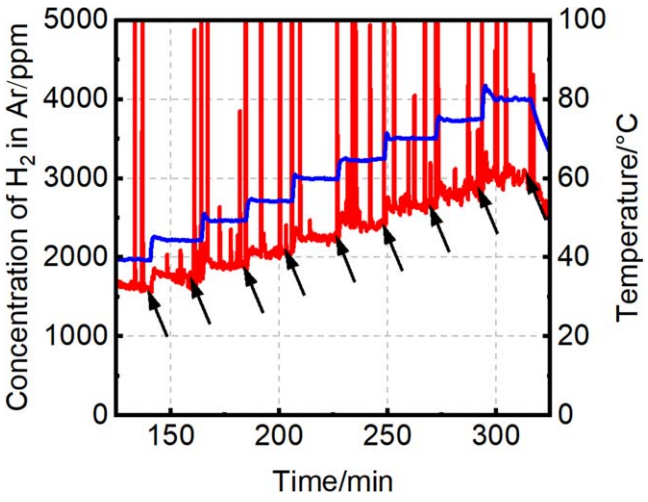

Figure 3. Concentration of hydrogen in argon for a N115 membrane. Color scheme: red line: hydrogen concentration, blue line: cell temperature. Black arrows indicate the values used to calculate the permeability. The periodic spikes in the permeate data at each set point originated from flushing the condensed water out of the gas dryer to prevent overflow into the gas analyzer.

displays the oxygen permeabilities. All tested membranes exhibit comparable permeability at a similar hydration state (wet or dry) for hydrogen as well as oxygen, which is consistent with literature.[34] Since permeability is an intrinsic material property, it is expected that membranes which only differ in thickness exhibit the same permeability values. Compared to the dry state, membranes have a higher permeability in the wet state. This can be attributed to an increased hydration level of the Nafion™ membrane, leading to an enhanced molecular mobility due to the plasticizing effect.[48] The increase of permeability by hydration is in the same order of magnitude for both hydrogen and oxygen permeabilities. In wet and dry states, permeability of hydrogen is higher than oxygen which can be attributed to hydrogen molecules being significantly smaller and lighter compared to oxygen molecules.[34] Due to higher hydrogen permeability, further experiments were only performed to explore hydrogen permeability through MEAs, as changes will be more pronounced. Figure 4 compares the (c) hydrogen and (d) oxygen permeability of water from literature[49,50] with that of

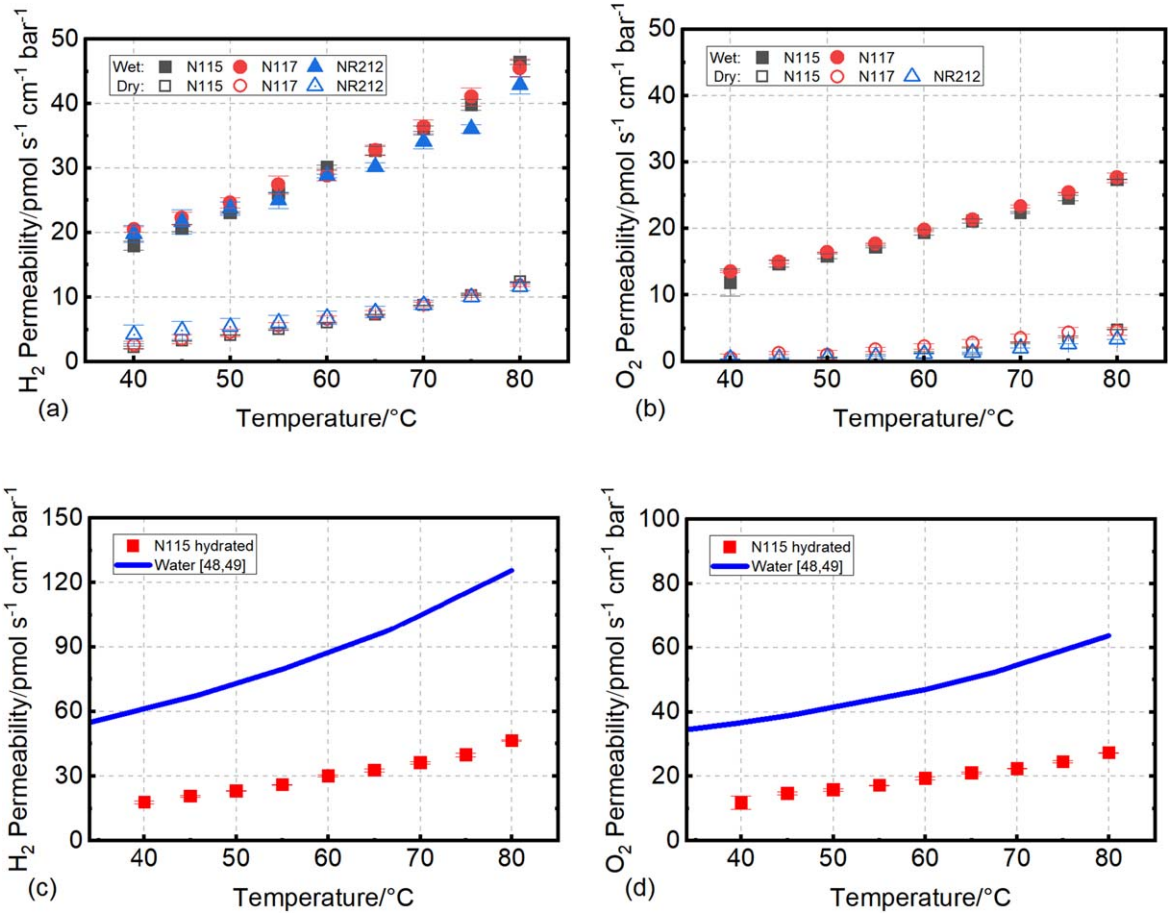

Figure 4. Hydrogen (a) and oxygen (b) permeability of different Nafion™ membranes in wet and dry state. The hydrated membrane N115 is compared to pure water for (c) hydrogen and (d) oxygen permeability. Water permeability was calculated by Ito et al.[49] with data from Wise et al.[50]

Nafion™ N115 acquired with the setup presented. As expected, pure water shows a higher permeability, as the diffusion through the membrane takes place in spatially limited water channels, that can be blocked by polymer chains inside the material.[34] Increasing the hydration of the membrane and widening the channels it is expected to also increase the gas permeability of the membrane, getting closer to that of pure water.

Looking at the impact of hydration on a dry membrane in Figs. 4a and 4b, an increase of permeability can be seen in Table II as a percentage. Here a significant difference can also be seen between both gases. Oxygen permeability has a more significant increase, after the membrane has been hydrated. This is due to oxygen being a diatomic molecule with about twice the size of that of hydrogen, thereby limiting its diffusive mobility inside the polymer.[51] When the membrane is hydrated, oxygen diffusion benefits more from the available water pathways. Distinct differences in slopes can be noticed in Figs. 4a and 4b when comparing the temperature effect on the permeability of a dry and wet membrane. This occurs because dry membranes facilitate diffusion only via the polymer phase, whereas wet membranes enable a mixed pathway of water and polymer. The pure polymer pathway is less temperature dependent, requiring more energy, while the pathway through water is activated with less energy.[34]

Table II. Comparison of hydrogen and oxygen permeability of Nafion™ N115, increase from a dry membrane to a hydrated membrane at a temperature range of 40 °C to 80 °C. Percentages indicate the relative increase of permeability from dry to hydrated.

	Increase of permeability from dry to wet	
Temperature	Hydrogen	Oxygen
°C		
40	804%	43155%
45	634%	5504%
50	554%	2693%
55	517%	2339%
60	494%	1358%
65	445%	1343%
70	414%	796%
75	386%	656%
80	374%	567%

A comparison with literature values and data obtained in this work is presented in Fig. 5. It is divided into (a) hydrogen permeability of a hydrated N115 membrane, (b) hydrogen permeability of a dry N115 membrane, (c) oxygen permeability of a hydrated N115 membrane and finally (d) oxygen permeability of a dry N115 membrane. The literature values were recorded using Nafion™ of different thicknesses, but since permeability is normalized to thickness, it can be read as an intrinsic material characteristic. Literature values show a strong dispersion, even though clear trends are visible. This could be from the usage of different measurement techniques, even though as an intrinsic material property the measurements should in theory be absolute values. One thing that could influence the difference between all measurements is how the membranes were conditioned before they were measured. This was not the same for all and was not always mentioned. Therefore, the impact of conditioning of N115 based membranes on its hydrogen permeability is crucial and will be discussed in detail in the following. The focus here is only on hydrogen, since the sensors

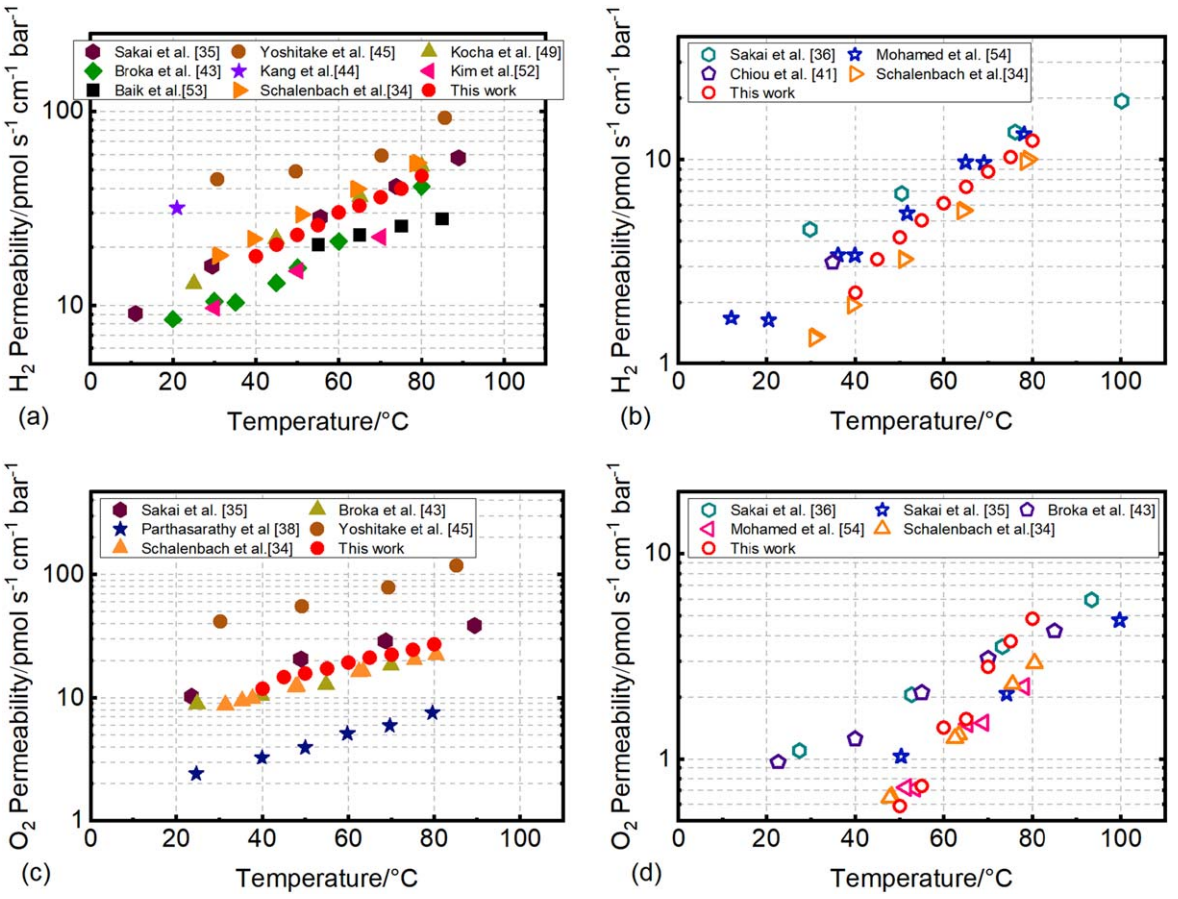

Figure 5. Literature overview of hydrogen and oxygen permeability of Nafion™ at different temperatures. Hydrogen permeability for hydrated[52–54] (a) and dry[55] (b) states of Nafion™, whereas oxygen permeability for hydrated (c) and dry (d) states of Nafion™. Red full circles indicate data from this work of a hydrated N115 membrane and red hollow circles indicate dry membrane.

are more sensitive to small changes. However, oxygen permeability should not be neglected, as it reduces gas production efficiency by recombination with hydrogen on the cathode. If oxygen is present on the cathode side, formation of H_2O_2 is possible, which could lead to radical formation that can degrade the polymer in the membrane.[25] Also, for processes in chemical industries that use the produced gases, gas purity can be an important factor.

Comparing the results of wet and dry measurements each for hydrogen and oxygen with that of Sakai et al.,[35,36] it can be noticed that the slope of the results seems nearly similar for both hydrated measurements. On the other hand, the permeabilities in the dry conditions demonstrate a clear difference and can be observed with a different slope. At lower temperatures the slope falls off with the setup of this work, which is more pronounced for dry oxygen. A likely cause for this is the sensitivity of the gas analyzers at low concentrations below 500 ppm, which is the case at lower end temperatures (< 60°C) with dry membranes. Especially for oxygen measurements, where the absolute amount of gas passing through the membrane is lower than that of hydrogen and due to the smaller thermal conductivity difference to argon, on which the detector relies. As fully dried out membranes are not used in PEMECs, this topic is not further investigated in the context of this study.

Since the literature values for permeability are typically recorded using pristine membranes and physio-chemical changes can already occur during the MEA production steps, the impact of catalyst coating on the permeability needs to be assessed in order to correctly assign possible changes to the applied conditioning procedures. To determine the influence of the MEA fabrication process on the hydrogen permeability of the membrane, a comparison of N115 membrane with N115-based MEA (both pre-treated ex situ in 80 °C water for 24 h) is presented in Fig. 6. A slight difference can be seen, mainly a marginal decrease in the slope of the MEA sample, indicating a slight decrease in diffusion process at higher temperatures. This could be due to two possible reasons: The electrodes coated onto the membrane are comprised of ionomer, catalyst and support material, thereby obviously changing the material properties and thickness of the sample. Furthermore, in a hot pressing or direct coating process of the membrane during MEA fabrication, the sample can undergo physical changes due to the applied temperature

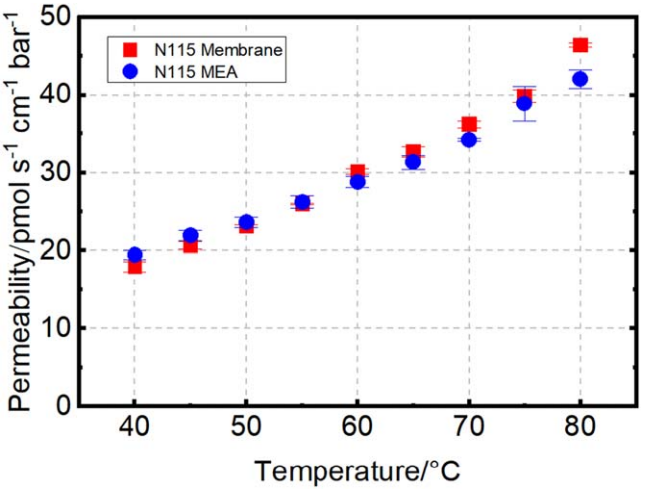

Figure 6. Comparison of hydrogen permeability of N115 membrane (red) and N115-based MEA (blue), pre-treated ex situ. Only a small change is visible, mainly to the slope.

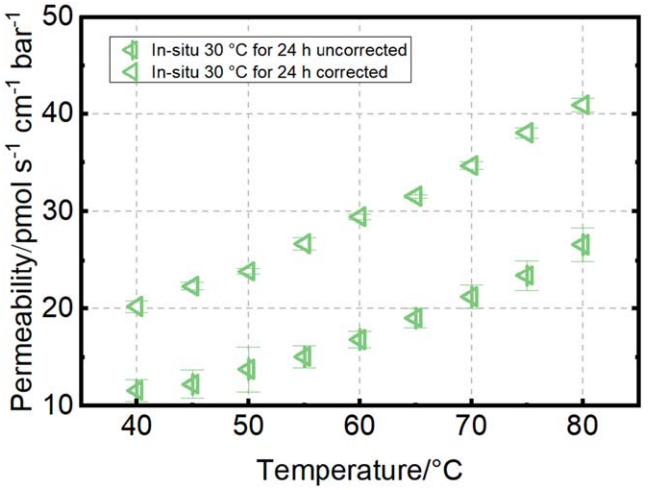

Figure 7. Hydrogen permeability of MEA 1 with uncorrected and corrected values. The difference arises from the in situ water pre-treatment, where the PTL pores can be blocked by water.

or chemical changes during the application of the catalyst ink. This can cause changes in the crystallinity or chemical structure of the membrane/ionomer.[56]

Owing to the distinct difference in hydrogen permeability of N115 membrane in wet and dry state and only marginal difference from N115-based MEA compared to pristine N115 membranes, MEAs were conditioned by pre-treating with DI-water at different temperatures for certain periods (see Table I). MEA 1 was assembled into the PEMEC in dry state and then flushed with 30 °C water for 24 h (in situ pre-treatment), after that the permeability was recorded. Here, it can be noticed that the measured permeability (Fig. 7) was greatly reduced for the in situ flushed samples compared with the ex situ wetted sample (Fig. 6).

The most likely reason for this measured stark decrease might be flooding of the PTL, where water is stuck inside the voids of the layer. The total diffusive flux Φ is dependent on the diffusion coefficient D, the concentration difference Δc between the two sides of the cell, and the distance d dividing the cell sides. Using Fick´s law of diffusion, the effect of PTL flooding on permeability can be explained:

$$\Phi = -D\frac{\Delta c}{d} \quad [2]$$

By filling the volume of the PTL with water during in situ pre-treatment, the gas diffusion process slows down considerably compared to ambient air filling the volume for the ex situ wetted samples. To correct this impact of PTL flooding, a correction value is implemented. To determine this value, a N115 membrane was conditioned in a beaker for an hour at 80 °C. Subsequently, the assembled cell's permeability was quantified in a temperature range of 40 °C to 80 °C. Afterwards, water was circulated through the same cell for a period of 5 min, and permeability experiments were repeated. The data from these tests, as presented in Table III, reveal a significant reduction in permeability after flushing it with water, showing that the water fills the voids within the PTLs, thereby hindering the hydrogen diffusion. Since the PTLs within the cells remained consistent across all tests, it can be assumed that the effect of the water filling the voids and increasing diffusion distance is comparable for all experiments. Consequently, the difference between the permeabilities before and after water pumping serves as a temperature-dependent correction value, which is applied to all MEAs subjected to conditioning via in situ pre-treatment or break-in. Equation 3 defines the corrected hydrogen permeability $\varepsilon_{H_{2,corr}}$, obtained by adding the correction value $\Delta\varepsilon_{H_2}(T)$ to the permeability value ε_{H_2} calculated from experimentally data.

Table III. Impact of in situ water exposure on hydrogen permeability of N115 membrane.

	Permeability		
Temperature	Without water	with water	Difference
°C	mol·s^{-1} cm^{-2} bar^{-1}	mol·s^{-1} cm^{-2} bar^{-1}	mol·s^{-1} cm^{-2} bar^{-1}
40	1.82E-11	4.45E-12	1.45E-11
45	2.17E-11	4.73E-12	1.69E-11
50	2.41E-11	6.20E-12	1.79E-11
55	2.70E-11	6.04E-12	2.10E-11
60	3.111E-11	7.30E-12	2.38E-11
65	3.37E-11	8.37E-12	2.53E-11
70	3.72E-11	8.84E-12	2.83E-11
75	4.09E-11	1.018E-11	3.07E-11
80	4.74E-11	1.501E-11	3.24E-11

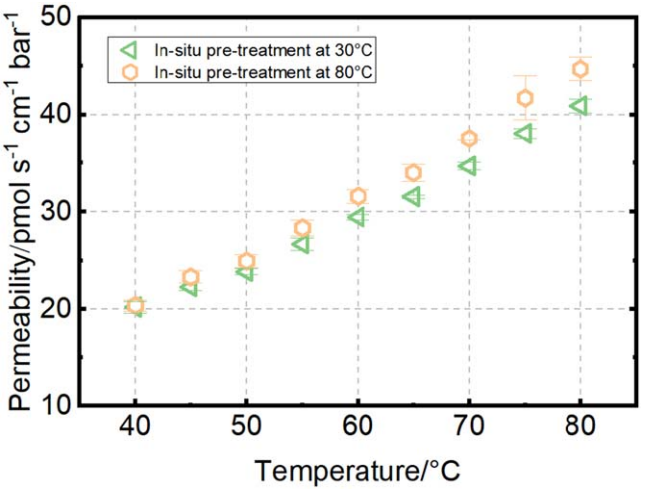

Figure 8. Effect of water temperature on hydrogen permeability as an in situ pre-treatment method (for 24 h) for MEA 1.

$$\varepsilon_{H_{2,corr}} = \varepsilon_{H_2} + \Delta\varepsilon_{H_2}(T) \quad [3]$$

To investigate the influence of pre-treatment temperature on the hydrogen permeability, MEA 1 was first pre-treated by flushing 30 °C water through the cell for 24 h and then recorded the hydrogen permeability. Subsequently, the procedure was replicated with 80 °C water. Figure 8 shows how the temperature increases during the in situ pre-treatment affects the hydrogen permeability of MEA 1. Here, the increase in pre-treatment temperature led to an overall increase in permeability. This is because the hydration level of Nafion™ is increased due to elevation in water content per sulfonic acid group at higher temperatures for the pre-treatment, which is in accordance with literature.[57]

Figure 9 shows a striking difference in hydrogen permeability of MEAs subjected to in situ pre-treatment (MEA 1) and ex situ pre-treatment (MEA 2 and 3). Even though all samples were treated with the water at the same temperature, a clear difference in permeability can be observed. This discrepancy can be attributed to the swelling behavior of Nafion™. When the membrane is confined within the PEMEC (along x- and *y*-axis), it mainly increases its thickness (*z*-axis) upon swelling. On the other hand, pre-treatment of MEAs in water without any constraints can result in membrane swelling in all possible dimensions.[58] This ultimately leads to differences when calculating permeability since the overall thickness of the

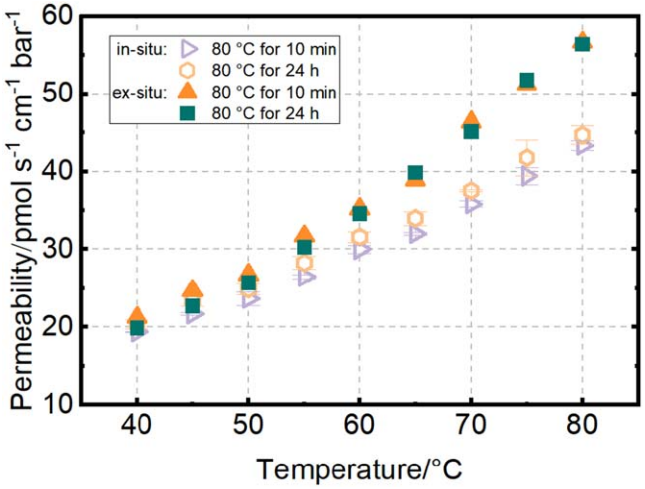

Figure 9. Hydrogen permeability of MEAs treated at 80 °C for either 10 min or 24 h. Hollow symbols represent in situ pre-treatment of MEA 1, while full symbols indicate ex situ pre-treatment of MEA 2 and 3. Choosing ex situ and in situ for pre-treatment influences permeability, while time at high temperatures has insignificant impact.

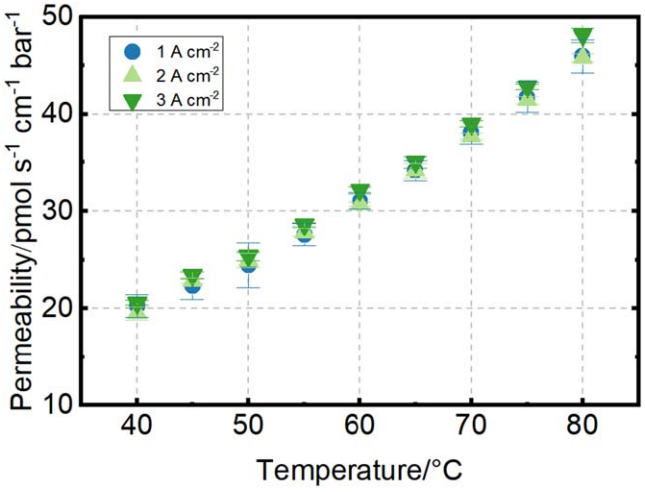

Figure 10. Hydrogen permeability acquired after break-in at different current densities for MEA 4. No significant change in hydrogen permeability is visible by increasing the current density.

membranes can differ depending on ex situ or in situ pre-treatment, that does not translate over to thickness measurements after cell disassembly. Also, the constrained swelling inside the cell assembly could put strain on the material and thereby changing the material properties. Additionally, by extending pre-treatment duration, hydrogen permeability increased, but relatively a little. This is because at elevated temperatures, the water activity increases, which speeds up the hydration time of the membrane.[32] For this reason, only a minor difference in hydration exists.

Another important consideration is the impact of the break-in process to activate MEAs by performing electrolysis as part of a conditioning procedure. To test the influence of the break-in process, the pristine MEA 4 was conditioned by applying 1 A cm^{-2}, 2 A cm^{-2} and 3 A cm^{-2} for 24 h each and the hydrogen permeability after each applied current density was measured. Figure 10 shows that increasing the current density influences the permeability only in a miniscule amount, specifically higher current density leads to slightly increased permeability.

Summary and Perspective

In this study, the gas permeability of membranes and membrane electrode assemblies (MEAs) used for proton exchange membrane electrolytic cells (PEMECs), pre- and post-operation was investigated. To corroborate the performance of the setup outlined in our recent work, the hydrogen and oxygen permeability of Nafion™-based membranes (N115, N117 and NR212) in dry and wet state were recorded. All membranes exhibited comparable permeabilities, demonstrating elevated values for oxygen and hydrogen permeability in the wet state, with hydrogen generally showing higher measured permeabilities. These findings were shown to be in good agreement with the available literature data. Only a slight difference in hydrogen permeability was observed between N115-based membranes and MEAs, indicating that the application of electrodes to the membrane might marginally affect the membrane properties.

Further investigations on MEA conditioning were conducted by pre-treating the MEA before (ex situ) and after (in situ) cell assembly, via in situ pre-treating MEA at elevated temperature 80° C and lowered temperature 30 °C, and by using several break-in procedures at varying current densities. The results indicate that ex situ pre-treatment of the MEA led to a clearly higher hydrogen permeability compared to in situ pre-treatment, due to the restricted swelling dimensions during in situ pre-treatment leading to possibly deviations in thickness and also might cause changes in the membrane material when swelling while confined inside of a PEMEC. Besides this effect, also elevated temperatures during conditioning lead to a higher hydrogen permeability, as well as break-in procedures applying current density and performing electrolysis, which resulted in a marginal increase in hydrogen permeability at higher current densities. Based on the impact of conditioning methods investigated in this study on the hydrogen crossover, the in situ pre-treatment of MEA at lower temperature and break-in at lower current density stand out most effective protocol. However, insights into its effect on the electrochemical performance of PEMEC and durability of cell components will pave the way to further optimize the performance of PEMEC. Since we only investigated N115-based MEA, an all-encompassing statement on the most effective conditioning procedure is challenging. The selection of the conditioning protocol strongly depends not only upon the employed MEA materials but also on the cell configurations; thus, the optimal protocol needs to be determined for each system separately.

These findings highlight the necessity of an experimental setup that enables in situ permeability measurements, as the distinct swelling behavior of Nafion™ outside of a constrained cell can introduce significant, non-negligible measurement errors. It also underlines the need for further gas permeability investigations in PEM electrolyzers, where the effect of conditioning and operation induced changes on the gas crossover need to be investigated in detail. This work demonstrates in-depth studies of gas permeability as a material parameter which will be further expanded upon in future works.

Acknowledgments

The authors gratefully acknowledge the financial support by the German Federal Ministry of Education and Research (BMBF) within the H2Giga project DERIEL (grant number 03HY122C).

ORCID

Leander Treutlein https://orcid.org/0009-0001-8989-5239
Ali Javed https://orcid.org/0000-0002-9947-0904
Niklas L. Wolf https://orcid.org/0009-0006-2834-5061
André Karl https://orcid.org/0000-0003-2289-5987
Eva Jodat https://orcid.org/0009-0004-8214-2981
Rüdiger-A Eichel https://orcid.org/0000-0002-0013-6325

References

1. European Commission, , *2050 long-term strategy* https://climate.ec.europa.eu/eu-action/climate-strategies-targets/2050-long-term-strategy_en (2019).
2. S. Dermühl and U. Riedel, *Fuel*, **340**, 127478 (2023).
3. M. Carmo, D. L. Fritz, J. Mergel, and D. Stolten, *Int. J. Hydrogen Energy*, **38**, 4901 (2013).
4. A. S. Aricò, S. Siracusano, N. Briguglio, V. Baglio, A. D. Blasi, and V. Antonucci, *J. Appl. Electrochem.*, **43**, 107 (2013).
5. Federal Ministry of Education and Research *Wasserstoff-Leitprojekte: H2Giga: serial production* https://www.wasserstoff-leitprojekte.de/projects/h2giga (2021).
6. A. Javed, N. L. Wolf, F. Meyer, L. Treutlein, H. Kungl, A. Karl, E. Jodat, and R.-A. Eichel, *Int. J. Hydrogen Energy*, **98**, 280 (2025).
7. A. Karl, E. Jodat, H. Kungl, and R. A. Eichel, *ECS Meeting Abstracts*, **MA2024-02**, 3198 (2024).
8. G. Papakonstantinou, G. Algara-Siller, D. Teschner, T. Vidaković-Koch, R. Schlögl, and K. Sundmacher, *Appl. Energy*, **280**, 115911 (2020).
9. E. Antolini, *ACS Catal.*, **4**, 1426 (2014).
10. M. Bernt, A. Hartig-Weiß, M. F. Tovini, H. A. El-Sayed, C. Schramm, J. Schröter, C. Gebauer, and H. A. Gasteiger, *Chem. Ing. Tech.*, **92**, 31 (2020).
11. S. Siracusano, N. Hodnik, P. Jovanovic, F. Ruiz-Zepeda, M. Šala, V. Baglio, and A. S. Aricò, *Nano Energy*, **40**, 618 (2017).
12. C. Heume et al., (2024) "Replication data for: cross-plane iridium-based filaments sap efficiency in proton exchange membrane electrolyzers." *Jülich DATA*.
13. T. Bystron, M. Vesely, M. Paidar, G. Papakonstantinou, K. Sundmacher, B. Bensmann, R. Hanke-Rauschenbach, and K. Bouzek, *J. Appl. Electrochem.*, **48**, 713 (2018).
14. C. Liu et al., *J. Electrochem. Soc.*, **170**, 34508 (2023).
15. Y. Pan, H. Wang, and N. P. Brandon, *J. Power Sources*, **513**, 230560 (2021).
16. J. Park, H. Oh, T. Ha, Y. I. Lee, and K. Min, *Appl. Energy*, **155**, 866 (2015).
17. S. A. Grigoriev, K. A. Dzhus, D. G. Bessarabov, and P. Millet, *Int. J. Hydrogen Energy*, **39**, 20440 (2014).
18. E. Kuhnert, M. Heidinger, D. Sandu, V. Hacker, and M. Bodner, "Analysis of PEM Water Electrolyzer Failure Due to Induced Hydrogen Crossover in Catalyst-Coated PFSA Membranes." *Membranes*, **13**, 3 (2023).
19. N. Norazahar, F. Khan, N. Rahmani, and A. Ahmad, *Int. J. Hydrogen Energy*, **50**, 842 (2024).
20. S. A. Grigoriev, V. I. Porembskiy, S. V. Korobtsev, V. N. Fateev, F. Auprêtre, and P. Millet, *Int. J. Hydrogen Energy*, **36**, 2721 (2011).
21. S. A. Grigoriev, V. N. Fateev, D. G. Bessarabov, and P. Millet, *Int. J. Hydrogen Energy*, **45**, 26036 (2020).
22. V. Karyofylli, Y. Danner, K. Ashoke Raman, H. Kungl, A. Karl, E. Jodat, and R.-A. Eichel, *J. Power Sources*, **600**, 234209 (2024).
23. B. Laoun and A. M. Kannan, *Int. J. Hydrogen Energy*, **85**, 440 (2024).
24. F. Fouda-Onana, M. Chandesris, V. Médeau, S. Chelghoum, D. Thoby, and N. Guillet, *Int. J. Hydrogen Energy*, **41**, 16627 (2016).
25. P. Frühwirt, A. Kregar, J. T. Törring, T. Katrašnik, and G. Gescheidt, *Phys. Chem. Chem. Phys.*, **22**, 5647 (2020).
26. L. Ghassemzadeh and S. Holdcroft, *JACS*, **135**, 8181 (2013).
27. S. Stucki, G. G. Scherer, S. Schlagowski, and E. Fischer, *J. Appl. Electrochem.*, **28**, 1041 (1998).
28. A. Weiß, A. Siebel, M. Bernt, T.-H. Shen, V. Tileli, and H. A. Gasteiger, *J. Electrochem. Soc.*, **166**, F487 (2019).
29. R. Omrani and B. Shabani, *Electrochim. Acta*, **377**, 138085 (2021).
30. S. A. Grigoriev, A. A. Kalinnikov, P. Millet, V. I. Porembsky, and V. N. Fateev, *J. Appl. Electrochem.*, **40**, 921 (2010).
31. M. N. I. Salehmin, T. Husaini, J. Goh, and A. B. Sulong, *Energy Convers. Manage.*, **268**, 115985 (2022).
32. G. Alberti, R. Narducci, and M. Sganappa, *J. Power Sources*, **178**, 575 (2008).
33. C. E. Evans, R. D. Noble, S. Nazeri-Thompson, B. Nazeri, and C. A. Koval, *J. Membr. Sci.*, **279**, 521 (2006).
34. M. Schalenbach, T. Hoefner, P. Paciok, M. Carmo, W. Lueke, and D. Stolten, *The Journal of Physical Chemistry C*, **119**, 25145 (2015).
35. T. Sakai, H. Takenaka, N. Wakabayashi, Y. Kawami, and E. Torikai, *J. Electrochem. Soc.*, **132**, 1328 (1985).
36. T. Sakai, H. Takenaka, and E. Torikai, *J. Electrochem. Soc.*, **133**, 88 (1986).
37. Z. Ogumi, Z. Takehara, and S. Yoshizawa, *J. Electrochem. Soc.*, **131**, 769 (1984).
38. A. Parthasarathy, S. Srinivasan, A. J. Appleby, and C. R. Martin, *J. Electrochem. Soc.*, **139**, 2530 (1992).
39. P. Trinke, P. Haug, J. Brauns, B. Bensmann, R. Hanke-Rauschenbach, and T. Turek, *J. Electrochem. Soc.*, **165**, F502 (2018).
40. P. Trinke, G. P. Keeley, M. Carmo, B. Bensmann, and R. Hanke-Rauschenbach, *J. Electrochem. Soc.*, **166**, F465 (2019).
41. J. S. Chiou and D. R. Paul, *Ind. Eng. Chem. Res.*, **27**, 2161 (1988).
42. F. Arena, J. Mitzel, and R. Hempelmann, *Fuel Cells*, **13**, 58 (2013).
43. K. BROKA and P. EKDUNGE, *J. Appl. Electrochem.*, **27**, 117 (1997).
44. Z. Kang, M. Pak, and G. Bender, *Int. J. Hydrogen Energy*, **46**, 15161 (2021).
45. M. Yoshitake, M. Tamura, N. Yoshida, and T. Ishisaki, "Studies of perfluorinated ion exchange membranes for polymer electrolyte fuel cells." *Denki Kagaku oyobi Kogyo Butsuri Kagaku*, **64**, 727 (1996).
46. L. Treutlein, A. Javed, H. Kungl, A. Karl, T. Hilche, E. Jodat, and R.-A. Eichel, *ChemRxiv* (2025), A versatile setup for determining the hydrogen and oxygen permeability of electrolyzer membranes and MEAs.
47. N. L. Wolf, A. Javed, L. Treutlein, H. Kungl, A. Karl, E. Jodat, and R.-A. Eichel, "Tuning Proton Exchange Membrane Electrolytic Cell Performance by Conditioning Nafion N115-Based Membrane Electrode Assemblies." *Electrochemical Science Advances*, **n/a**, e202400038 (2024).
48. Y. Hirata, Y. Miura, and T. Nakagawa, *J. Membr. Sci.*, **163**, 357 (1999).
49. H. Ito, T. Maeda, A. Nakano, and H. Takenaka, *Int. J. Hydrogen Energy*, **36**, 10527 (2011).
50. D. L. Wise and G. Houghton, *Chem. Eng. Sci.*, **21**, 999 (1966).
51. A. F. Ismail, "Polymeric and Inorganic." *Gas Separation Membranes* (Springer, Cham) (2015), International Publishing AG3319010956.
52. S. S. Kocha, J. Deliang Yang, and J. S. Yi, *AIChE J.*, **52**, 1916 (2006).
53. S. Kim, B. T. D. Nguyen, H. Ko, M. Kim, K. Kim, S. Nam, and J. F. Kim, *Int. J. Hydrogen Energy*, **46**, 15135 (2021).
54. K. D. Baik, B. K. Hong, and M. S. Kim, *Int. J. Hydrogen Energy*, **38**, 8927 (2013).
55. H. F. Mohamed, K. Ito, Y. Kobayashi, N. Takimoto, Y. Takeoka, and A. Ohira, *Polymer*, **49**, 3091 (2008).
56. J. E. Hensley, J. D. Way, S. F. Dec, and K. D. Abney, *J. Membr. Sci.*, **298**, 190 (2007).
57. Y. Liu, J. L. Horan, G. J. Schlichting, B. R. Caire, M. W. Liberatore, S. J. Hamrock, G. M. Haugen, M. A. Yandrasits, S. Seifert, and A. M. Herring, *Macromolecules*, **45**, 7495 (2012).
58. M. Carmo, D. Henkensmeier, W. Lüke, and D. Stolten, *ECS Meeting Abstracts*, **MA2015-02**, 1515 (2015).